Chinese Chemical Letters 31 (2020) 145–149

Contents lists available at ScienceDirect

Chinese Chemical Letters

journal homepage: www.elsevier.com/locate/cclet

Communication

Dual functional AgNPs-M13 phage composite serves as antibacterial film and sensing probe for monitoring the corrosion of chromium-containing dental alloys

Ting Yang[a,*], Na Li[a], Xiaoyan Wang[a], Jian Zhai[a], Bo Hu[b], Mingli Chen[a], Jianhua Wang[a,*]

[a] Research Center for Analytical Sciences, Department of Chemistry, College of Sciences, Northeastern University, Shenyang 110819, China
[b] Department of Biochemistry and Molecular Biology, School of Life Sciences, China Medical University, Shenyang 110122, China

ARTICLE INFO

Article history:
Received 19 April 2019
Received in revised form 10 July 2019
Accepted 10 July 2019
Available online 11 July 2019

Keywords:
AgNPs-M13 phage composite
Green preparation
Bactericidal activity
Colorimetric sensing
Cr(III)

ABSTRACT

The preparation of silver nanoparticles (AgNPs) with microbe or plant tissues as bio-template offers green approach, while it suffers from low harvest and purification is needed. Herein, we propose a facile protocol for one-pot preparation of AgNPs using M13 phage as bio-template by simply mixing $AgNO_3$ solution with alkali M13 phage. In the obtained AgNPs-M13 phage composite, Cr(III) selectively coordinates with the amino residues on phage surface and leads to the aggregation of AgNPs through the bridging of M13 phages. This makes it feasible for colorimetric sensing of Cr(III) by measuring the absorbance ratio of AgNPs at 600 and 405 nm, which provides a LOD of 14 nmol/L. The composite also showed favorable bactericidal activity for both Gram-positive and Gram-negative bacteria, making it a promising candidate as antibacterial film in chromium-containing dental alloys and meanwhile serve as a sensing probe for monitoring the corrosion of the dental alloys.

The versatility and unique characteristics of silver nanoparticles (AgNPs) have attracted remarkable research attention due to its well-known broad-spectrum antimicrobial activity [1], plasmonic activity [2] and catalytic properties [3]. The intense applications of AgNPs in biological field inspired researches to integrate green chemistry approaches to prepare AgNPs using biological substances as templates [4,5]. Numerous biological sources, including bacteria [6], yeast [7], fungi [8] and plant extracts [9], were reported as bio-templates for the preparation of AgNPs. However, the most obstacles for the biogenic AgNPs prepared by microorganisms is the harvest and purification issues, whereas the indeterminate components of plant extracts between different batches hindered the scale-up production of AgNPs with uniformed properties [10]. Hence, green synthesis of AgNPs with batch reproducibility and easy treatment procedure is required.

M13 phage is a filamentous bacteriophage with a nanoscale dimension of 6.5 nm in width and 900 nm in length. Its surface is assembled by ~2700 units of highly ordered major capsid protein with a spiral structure, forming a rigid proteinous cylinder coat [11]. M13 phage is harmless to humans since it specifically infects its host bacteria and can be inexpensively purified in large quantity [12]. The well-defined structure and the precisely fixed location of reactive sites (amino residues) ensure the reproducibility of the chemical modification of M13 phage surface [13]. M13 phages can work as biological reducing agents to achieve direct reduction of metal ions, since abundant reductive amino acid residues including tyrosine, tryptophan, cysteine, aspartic acid and glutamic acid are present on M13 phage surfaces [14]. Leong *et al.* reported that the bio-reduction of chloroauric acid into gold nanoparticles by a wild type of M13 phage in acid and neutral conditions can be accomplished at 37 °C within 24 h [15], while our group recently found that in basic condition the formation of gold nanoparticles can be accelerated within 90 min at room temperature [16]. By expressing tetra glutamic acid peptide on the tips of the major capsid protein of M13 phage, Ag^+ can also be reduced and deposited on the surface of M13 phages to form silver nanowires [17]. Nevertheless, the biosynthesis of silver nanoparticles using wild type of M13 phage (without genetic engineering) has not been reported yet, probably due to the insufficient reducing ability of M13 phage at neutral conditions.

Chromium is a metallic element that is widely used in various industries, with metal alloys account for ~85% of the chromium usage [18]. For instance, chromium containing alloy, such as Co-Cr-Mo alloy is widely used for the fabrication of dentures for their suitable mechanic property and low cost [19]. However, the release

* Corresponding authors.
E-mail addresses: yangting@mail.neu.edu.cn (T. Yang), Jianhuajrz@mail.neu.edu.cn (J. Wang).

https://doi.org/10.1016/j.cclet.2019.07.026
1001-8417/

of chromium ions due to the corrosion of these dental alloys is also a concerned issue. Chromium is toxic and carcinogenic even at low dosage in the form of Cr(VI), whereas Cr(III) may also cause genomic instability and cell mutation once over-ingested [20]. Therefore, it is necessary to develop a facile approach to indicate the corrosion of dental alloy and the corresponding chromium release. Colorimetric method offers such choice, with these based on gold/silver nanoparticles most attractive and sensitive with detection limits ranging from 0.4 nmol/L to 6.25 μmol/L (Table S1 in Supporting information).

In this work, we demonstrated that AgNPs can be easily obtained using wild type of M13 phage as bio-template at basic conditions without heating or additional reductants. AgNPs with an average size of 26 nm scattered in the network formed by the tethering of M13 nanofibers. The AgNPs-M13 phage composites can be directly used for further application without extra modification and purification. The coordination of Cr(III) by the amino residues on the surface of M13 phages induces aggregation of AgNPs through the bridging of M13 phages. The AgNPs-M13 phage composites showed a high selectivity towards Cr(III). A colorimetric detection method for Cr(III) was thus developed, which was successfully applied in Cr(III) analysis in a series of environmental water samples. Meanwhile, the composites also showed good bactericidal activity for both Gram-positive and Gram-negative bacteria. This versatile composites are expected to play a special role both as antibacterial film for chromium-containing dental alloys and the sensing probe for the corrosion of these alloys.

Preliminary experiments indicated that wild type of M13 phage cannot reduce Ag^+ to AgNPs at acidic or neutral conditions. This observation is in accordance with previously reported results [17] (Fig. S1A in Supporting information). However, by simply mixing $AgNO_3$ solution with M13 phage and NaOH solution at 37 °C, the formation of plenty of AgNPs crystals was found, which results in an obvious color change from colorless to brown. Fig. S1A illustrated a clear increment on the yield of AgNPs with the increase of pH values within a range of pH 2.7 – 12. At a higher pH value, the SPR absorption band of AgNPs becomes sharper, illustrating more uniformed size distribution. It is reported that pH strongly influences the dissociation state and the redox state of both the binding/reducing site on the surface of M13 phage and Ag^+ [15,21]. Considering the fact that the isoelectric point of M13 phage is around pH 4.4, when pH value of the reaction system is lower than 4.4 [22], the protonation of amine groups in the capsid protein leads to a positively charged surface, making it hard to bind with Ag^+ due to the electrostatic repulsion. With the increase of pH values, the surface charge of M13 phage becomes negative along with the improvement on the reduction capability of the capsid protein, which facilitates the binding of Ag^+ and the subsequent reduction of Ag^+ to AgNPs on the phage surface [23]. The increased concentration of M13 phage can also boost the yield of AgNPs, as shown in Fig. S2 (Supporting information). After a brief screening of the reaction ratio between Ag^+ and M13 phages, the optimized initial concentration of Ag^+ and M13 phages in the reaction system were set to be 10 mmol/L and 3.23×10^{12} pfu/mL, respectively. Considering that the extremely basic condition is not suitable for conducting bactericidal studies, pH 10.20 was chosen for the bio-reduction process, and the complete reduction takes 12 h at 37 °C (Fig. S3 in Supporting information). As illustrated in Fig. S1A, the incubation of 3.23×10^{12} pfu/mL of M13 phages with 10 mmol/L of $AgNO_3$ solution (adjusting to pH 10.20 by NaOH) for 12 h provides high yield of brown AgNPs with λ_{max} 405 nm. AFM image shows that M13 phages and silver nanoparticles form a network structure, in which the silver nanoparticles are partially bound with the filamentous structure of the M13 phage (Fig. S1B in Supporting information).

XPS spectrum showed two binding energy peaks of Ag 3d centered at 367.9 and 373.9 eV, suggesting that the AgNPs are mainly composed of Ag^0 [24] (Fig. S1C in Supporting information). TEM image indicated that the as-prepared AgNPs are approximately spherical in shape and about 26 nm in diameter (Fig. S1D in Supporting information). Zeta potential measurement results showed that the composite is negatively charged (−7.63 mV), which is caused by the negative charge of M13 bacteriophage under alkaline environment.

Strains of *E. coli*, *P. aeruginosa*, *S. aureus* and *B. subtilis* were used to evaluate the bactericidal capability of AgNPs-M13 phage composite. Fig. 1A shows the viability of the four bacterial species at $\sim 10^7$ cfu/mL incubated with 86.4 μg/mL of the composite for different time intervals. It is obvious that the AgNPs-M13 phage composite can effectively reduce the viability of all four bacterial species in a time-dependent manner. The viability of the four species decreases with the increase of the incubation time, and all the species lost their viability within 15 min. Notably, *B. subtilis* seems to be more susceptible to the AgNPs-M13 phage composite, as 100% killing rate is observed within 2 min (Fig. 1A).

The dose-dependent bactericidal behavior of the AgNPs-M13 phage composite was tested by incubating $\sim 10^7$ cfu/mL of the four types of bacterial species with different concentrations of the composite for 10 min, and the results are shown in Fig. 1B. Over 91.4% of *B. subtilis* (1.38×10^7 cfu/mL) can be killed by the composite at a dosage of 1.4 μg/mL, whereas at a same incubation time, the viability of the other three species remain at 64.3% (*E. coli*), 88.8% (*P. aeruginosa*) and 90.5% (*S. aureus*), respectively. It is obvious that 21.6 μg/mL of the composite results in a 100% killing rate for *B. subtilis*, whereas a minimum concentration of 86.4 μg/mL for AgNPs-M13 composite is required to achieve 100% killing rate for *E. coli*, *P. aeruginosa* and *S. aureus*.

The oxidative stress has been reported as a common mechanism of antibacterial activity of AgNPs [25,26]. The interaction of AgNPs with bacterial cells often produces reactive oxygen species (ROS) and induces oxidative stress in the cells which causes damages to the proteins and nucleic acids. A fluorescent probe DCFH-DA was used to evaluate the intracellular ROS level after treated with AgNPs-M13 phage composite. DCFH-DA itself exhibits no fluorescence but forms green fluorescent dichlorofluoroscein (DCF) once oxidized by ROS species [25]. As shown in Figs. S4A and B (Supporting information), after treated with AgNPs-M13 phage composite, all the four species exhibit obvious green fluorescence, while virtually no fluorescence is observed in the absence of AgNPs-M13 phage composite. The intracellular ROS induced by AgNPs are basically in the same level for all four bacterial species, indicating the reactive oxidative species play a key role in the bactericidal function of the AgNPs-M13 phage composite.

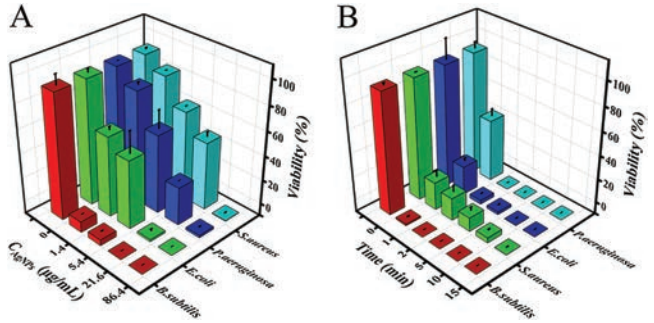

Fig. 1. (A) The viability of the four bacterial species as a function of incubation time after treated with 86.4 μg/mL of AgNPs-M13 phage composite. (B) The viability of the four bacterial species as a function of the concentration of AgNPs-M13 phage composite after treated with the composite for 10 min.

Propidium iodide (PI) staining test was further conducted to confirm the disruption of the bacterial cell membrane by the composite. PI is a membrane-impermeable fluorescent dye and only those with damaged membranes can be stained with PI. An increase in PI fluorescence intensity indicates damage to the cytoplasmic membrane [27]. Figs. S5A and B (Supporting information) illustrated intensive fluorescence after the bacterial cells are treated with AgNPs-M13 phage composite, whereas virtually no fluorescence is produced by the bare bacteria cells, indicating that the addition of AgNPs-M13 phage composite causes obvious damage for the cytoplasmic membrane of all the four species. In comparison with *S. aureus* and *B. subtilis*, larger populations of PI-stained cells are observed in the case of *E. coli* and *P. aeruginosa.* Since they are both Gram-negative bacteria, their cell walls are only composed of thin peptidoglycan layer which is prone to be attacked by AgNPs [28].

SEM microscopy was applied to evaluate the morphology changes of the native bacterial cells and bacterial cells treated with the AgNPs-M13 phage composite (Fig. 2). As shown in Figs. 2A1-D1, the native bacterial cells are smooth and intact. After treated with AgNPs-M13 phage composite, the cell wall become wrinkled and serious deformation of the cell shape is observed in the case of *P. aeruginosa* (Fig. 2C2) and *E. coli* (Fig. 2D2), indicating the cell membrane is disrupted and lost its original barrier function. In contrast, the surface of *S. aureus* and *B. subtilis* cells exhibited only minor deformation (Figs. 2A2 and B2). It is also worth noting that the surface for *B. subtilis* cells is thickly covered with AgNPs, which might be the results of the special interaction between the surface components of *B. subtilis* with AgNPs-M13 phage composite [29].

We further evaluated the colorimetric Cr(III) sensing performance by mixing 20 μL of series concentrations of Cr(III) standard solutions with 80 μL of AgNPs-M13 phage composite at room temperature. Upon the addition of Cr(III) into the AgNPs-M13 phage composite solution, an immediate aggregation of AgNPs occurs, resulting in a color change from yellow to light pink within a few seconds. UV–vis absorption spectra for the mixtures in Fig. 3A illustrated that with the increase of Cr(III) concentration, an obvious decrement is encountered for the SPR absorption peaks of AgNPs at 405 nm, and meanwhile a new absorption peak at 600 nm is observed. The dynamic light scattering (DLS) results indicated that the hydrodynamic diameter of AgNPs increases with the increase of Cr(III) concentration (Fig. 3B), and meanwhile the corresponding TEM image showed more aggregated AgNPs (Figs. 3C – E), which is in accordance with the results as achieved by UV–vis absorption spectra. It is worth noting that the more aggregated AgNPs, the more bare M13 phage fibers are observed in the TEM images. In other words, it is quite possible that the competitive binding of amino residues on the surface of M13 phage by Cr(III) leads to the stripping of AgNPs from the surface of M13 phages, resulting in the aggregation of un-protected AuNPs. According to HSAB theory, Cr(III) is considered as hard acid which binds preferentially with hard bases including R-OH, R-NH_2 [30]. As there are sufficient carboxyl group and amine group on the proteinous surface of M13 phage, it can provide favorable binding capability towards Cr(III).

The selectivity for Cr(III) assay was ascertained by replacing Cr(III) with other potential interfering ions by following the analyzing procedure. As can be seen in Fig. 4A and Fig. S6 (Supporting information), the commonly encountered metal cations including Na^+, K^+, Mg^{2+}, Ca^{2+}, Ba^{2+}, Cr(VI), Mn^{2+}, Fe^{3+}, Al^{3+}, Co^{2+}, Ni^{2+}, Cu^{2+}, Zn^{2+}, Cd^{2+}, Hg^{2+} and Pb^{2+} pose no obvious response to the AgNPs-M13 phage composite, confirming the high selectivity for Cr(III) detection.

The absorbance ratio at 600 nm and 405 nm (A_{600}/A_{405}) is proportional to the concentration of Cr(III), thus was used for the quantification of Cr(III) (Fig. 4B). In order to obtain better analytical performance, some of the key parameters concerning Cr(III) sensing were optimized (see details in the Supporting information), including pH value of the solution and the incubation time. The sensing system reaches equilibrium after 30 min (Fig. S7 in Supporting information) and achieves maximum response towards Cr(III) at pH 7 – 8 (Fig. S8 in Supporting information). Under optimized conditions, the detection limit for Cr(III) was calculated to be 14 nmol/L (3σ/k, $n = 11$), within a linear range of 0.02 – 0.50 μmol/L. The detection limit is far below the current standard stipulated by U.S. Environmental Protection Agency (1.9 μmol/L) [25], indicating that this sensing assay can be potentially applied for the Cr(III) determination in aqueous media.

The composites were further applied for the measurement of Cr (III) content in Co-Cr dental alloy and Ni-Cr dental alloy, and the analysis results listed in Table S2 (Supporting information) are in accordance with the standard value provided by the manufacturer's instructions. Spiking recovery studies were performed by adding known concentrations of Cr(III) (0.10, 0.50 μmol/L) to aqueous samples and the total amount of Cr(III) was determined with the proposed method. The recoveries are derived to be within 83%–105% (Table S3 in Supporting information). These results validated the reliability and practicability of the proposed colorimetric method for Cr(III) detection.

We also tried to monitor chromium release from Co-Cr and Ni-Cr dental alloys due to their corrosion in the medium of saliva. The dental alloys were first immersed into artificial saliva for one week to facilitate corrosion and chromium release. Thereafter the Cr(III) content was determined by using the developed method. The experimental results indicated that the corrosion and release of chromium from the alloys into saliva is a pretty slow process, and thus the concentration of the released Cr(III) in saliva is below the detection limit of the present colorimetric approach, Thus,

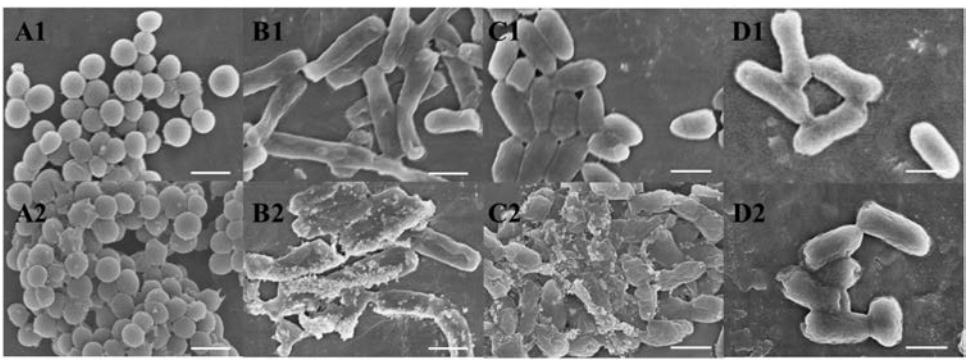

Fig. 2. SEM images of the four bacterial species before (A1, B1, C1, D1) and after (A2, B2, C2, D2) the addition of AgNPs-M13 phage composite. *S. aureus* (A1, A2); *B. subtilis* (B1, B2); *P. aeruginosa* (C1, C2); *E. coli* (D1, D2); Scale bar: 1 μm.

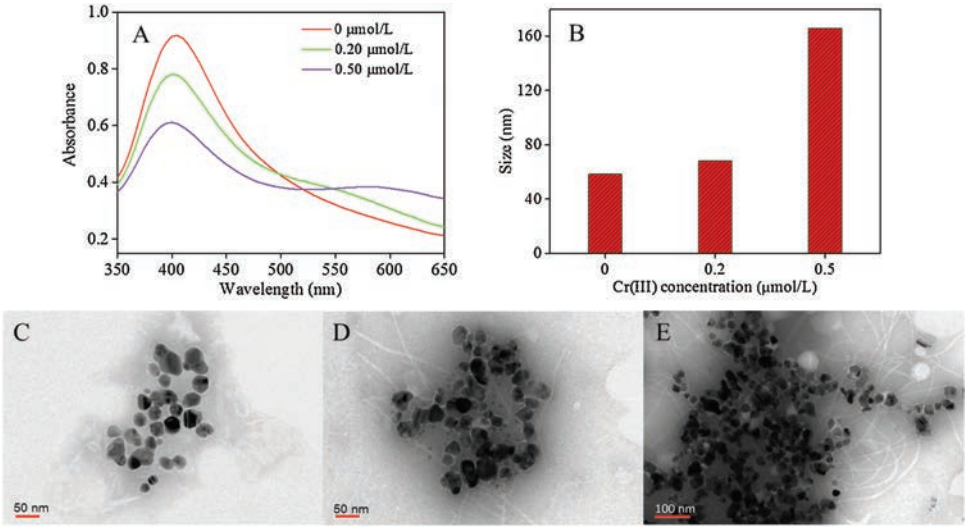

Fig. 3. (A) UV–vis absorption spectra, (B) hydrodynamic diameter and (C–E) TEM images of AgNPs-M13 phage composite with/without the addition of Cr(III). C: without Cr(III); D: added 0.20 μmol/L Cr(III); E: added 0.50 μmol/L Cr(III). Phages were negatively stained by phosphotungstic acid.

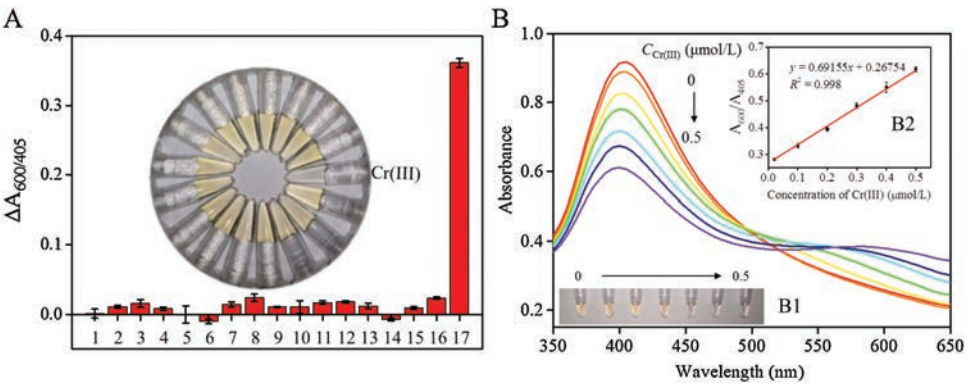

Fig. 4. (A) Selectivity studies of the AgNPs-M13 phage composite towards Cr(III). Concentrations of metal ions are listed as: 1. Na^+, 2. K^+, 3. Mg^{2+}, 4. Ca^{2+}, 5. Ba^{2+}, 7. Mn^{2+}, 9. Co^{2+}, 10. Ni^{2+}, 13. Cd^{2+}: 10.00 μmol/L; 6. Cr(VI), 11. Cu^{2+}, 12. Zn^{2+}, 14. Hg^{2+}: 4.00 μmol/L; 8. Fe^{3+}: 3.00 μmol/L; 16. Pb^{2+}: 1.00 μmol/L; 15. Al^{3+}, 17. Cr(III): 0.40 μmol/L. The inset shows the color photograph of the corresponding solutions. (B) UV–vis absorption spectra of the AgNPs-M13 phage composite with the addition of Cr(III) with various concentrations (0, 0.02, 0.10, 0.20, 0.30, 0.40, 0.50 μmol/L). Inset B1 shows the color photograph of the corresponding solutions. Inset B2 shows the response of absorbance ratio (A_{600}/A_{405}) of the colorimetric assay system *versus* Cr(III) concentrations.

Cr(III) standard solutions were spiked into the lixiviums to simulate lixiviums with a long-term corrosion and release of Cr(III). The analysis results were given in Table S4 (Supporting information), where recoveries within the range of 94%–106% were illustrated. This observation clearly demonstrated the promising potential of the AgNPs-M13 phage composite for probing/monitoring the corrosion of chromium-containing dental alloys.

In summary, a green strategy for the synthesis of AgNPs using wild type of M13 phage as bio-template was developed. M13 phages were employed both as reductants and capping agents. The preparation procedure was purification-free. The resulting AgNPs-M13 phage composite selectively respond to Cr(III), which was further used for the colorimetric detection of Cr(III). In addition, the composite also showed good bactericidal activity for both Gram-positive and Gram-negative bacteria. Considering that some of the dental alloy materials contain high levels of chromium which are prone to be more corrosive with dental bacterial plaque adhered on their surface, and the extent of their corrosion can be reflected by the leakage of Cr(III) ions, the AgNPs-M13 phage composite can potentially be used both as antibacterial film for these dental alloys and the sensing probe for monitoring and tracing their corrosion process.

Acknowledgments

Financial support from the National Natural Science Foundation of China (Nos. 21874014, 21727811, 21675019, 21605161), the Fundamental Research Funds for the Central Universities (No. N180505021) are highly appreciated.

Appendix A. Supplementary data

Supplementary material related to this article can be found, in the online version, at doi:https://doi.org/10.1016/j.cclet.2019.07.026.

References

[1] C. Liu, S. Han, S. Wang, et al., Chin. Chem. Lett. 29 (2018) 1824–1828.
[2] S. Linic, P. Christopher, D.B. Ingram, Nat. Mater. 10 (2011) 911–921.
[3] C. Wen, A.Y. Yin, W.L. Dai, Appl. Catal. B -Environ. 160 (2014) 730–741.
[4] T. Klaus-Joerger, R. Joerger, E. Olsson, C.G. Granqvist, Trends Biotechnol. 19 (2001) 15–20.
[5] N. Saifuddin, J. Chem. 6 (2009) 61–70.
[6] D. Bhatt, E. Gupta, S. Kaushik, et al., IET Nanobiotechnol. 12 (2018) 981–986.
[7] F.A. Cunha, M. Cunha, S.M. da Frota, et al., World J. Microb. Biot. 34 (2018) 127–142.
[8] B.A. Omran, H.N. Nassar, N.A. Fatthallah, et al., J. Appl. Microbiol. 125 (2018) 370–382.
[9] A. Massironi, A. Morelli, L. Grassi, et al., Carbohyd. Polym. 203 (2019) 310–321.

[10] H. Korbekandi, S. Iravani, S. Abbasi, Crit. Rev. Biotechnol. 29 (2009) 279–306.
[11] G.P. Smith, V.A. Petrenko, Chem. Rev. 97 (1997) 391–410.
[12] C. Mao, A. Liu, B. Cao, Angew. Chem. Int. Ed. 48 (2009) 6790–6810.
[13] J.M.L. Bernard, M.B. Francis, Front. Microbiol. 5 (2014) 1–7.
[14] W.J. Chung, D.Y. Lee, S.Y. Yoo, Int. J. Nanomed. 9 (2014) 5825–5836.
[15] M.I. Setyawati, J. Xie, D.T. Leong, ACS Appl. Mater. Interfaces 6 (2014) 910–917.
[16] X. Wang, T. Yang, X. Zhang, et al., Nanoscale 9 (2017) 16728–16734.
[17] K.T. Nam, Y.J. Lee, E.M. Krauland, et al., ACS Nano 2 (2008) 1480–1486.
[18] R.D. Morrison, B.L. Murphy, Environmental Forensics: Contaminant Specific Guide, Academic Press, Burlington, 2010.
[19] T. Puskar, D. Jevremovic, R. Williams, et al., Materials 7 (2014) 6486.
[20] P. Biswas, A.K. Karn, P.G. Kale, P. Balasubramanian, Biosens. Bioelectron. 94 (2017) 589–604.
[21] Y. Ji, H. Gao, J. Sun, F. Cai, Chem. Eng. J. 172 (2011) 122–128.
[22] J. Rong, L.A. Lee, K. Li, et al., Chem. Commun. (2008) 5185–5187.
[23] J.P. Xie, Y.G. Zheng, J.Y. Ying, J. Am. Chem. Soc. 131 (2009) 888–889.
[24] A.M. Ferraria, S. Boufi, N. Battaglini, et al., Langmuir 26 (2010) 1996–2001.
[25] B. Ramalingam, T. Parandhaman, S.K. Das, ACS Appl. Mater. Interfaces 8 (2016) 4963–4976.
[26] O. Choi, Z. Hu, Environ. Sci. Tech. 42 (2008) 4583–4588.
[27] X. Tian, X. Jiang, C. Welch, et al., ACS Appl. Mater. Interfaces 10 (2018) 8443–8450.
[28] J. Wang, C. Chen, Biotechnol. Adv. 27 (2009) 195–226.
[29] K. Rasool, M. Helal, A. Ali, et al., ACS Nano 10 (2016) 3674–3684.
[30] R.G. Pearson, J. Chem. Educ. 45 (1968) 581–587.